Macromolecules

pubs.acs.org/Macromolecules Article

Synthesis and Chemical Transformation of Nitrogen-Rich Polyolefins through Copolymerization of Ethylene with Polar Cyclic Olefins

Kangkang Li, Lei Cui, Yixin Zhang,* and Zhongbao Jian*

Cite This: *Macromolecules* 2025, 58, 9412−9419 Read Online

ACCESS | Metrics & More | Article Recommendations | Supporting Information

ABSTRACT: Direct coordination−insertion copolymerization of ethylene with polar monomers provides an atom- and energy-efficient route to functionalized polyolefins. However, the incorporation of nitrogen-containing comonomers into polyolefins remains problematic due to nitrogen-induced catalyst poisoning. Herein, two highly strained bicyclic nitrogen-containing comonomers (aminooxy-embedded norbornene: $\mathbf{NB_{NO}}$, aza-embedded norbornene: $\mathbf{NB_{NN}}$) are introduced, which effectively diminish the catalyst poisoning propensity. The copolymerization of ethylene with $\mathbf{NB_{NO}}$ results in the formation of poly(E-$\mathbf{NB_{NO}}$) with high comonomer incorporation of 38.3 mol %. Likewise, the reaction with $\mathbf{NB_{NN}}$ produces poly(E-$\mathbf{NB_{NN}}$), which possesses both high molecular weight of 108.1 × 10^3 g mol^{-1} and high comonomer incorporation of 28.3 mol %. By adjusting the concentration of $\mathbf{NB_{NN}}$, the semicrystalline poly(E-$\mathbf{NB_{NN}}$) (T_m = 126−127 °C) is transformed into the amorphous, transparent, optical poly(E-$\mathbf{NB_{NN}}$) (T_g = 60−132 °C; transmittance = 95.2−96.6% at 400 nm). Notably, poly(E-$\mathbf{NB_{NO}}$) undergoes N−O reductive cleavage, giving bifunctional poly(E-NH−OH) that features both −OH and −NH moieties. Poly(E-$\mathbf{NB_{NN}}$) is transformed into an azo-containing polyolefin [poly(E-N═N)]. Precise modulation of the N_2-extrusion conditions in poly(E-N═N) enables the formation of diverse all-hydrocarbon cyclo-containing polyolefin architectures, which are difficult to access by other methods. This work circumvents conventional nitrogen-induced deactivation and provides a versatile platform for the synthesis and transformation of nitrogen-functionalized polyolefins.

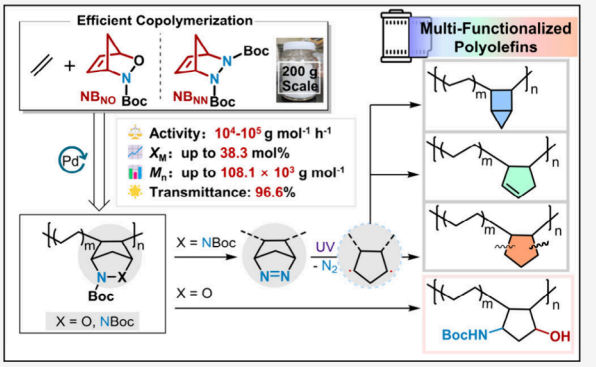

INTRODUCTION

Polyolefins are the most widely produced plastics in the world owing to their notable properties. Transition-metal-catalyzed coordination−insertion polymerization of simple olefins (e.g., ethylene, propylene) has been extensively explored.[1−4] Nevertheless, the direct copolymerization of olefins with polar olefinic monomers remains challenging, given that polar functionalities always poison transition-metal catalysts.[5−10] Since the seminal works from Brookhart and Drent, d^8 Ni(II) and Pd(II) catalysts, owing to their reduced oxophilicity, have efficiently promoted the copolymerization of various polar olefins with nonpolar olefins, affording functionalized polyolefins.[11−18]

Among polar comonomers, the exploration of oxygen-containing olefinic monomers including most acrylates and a few vinyl ethers and vinyl acetates has been most extensive due to their functional diversity and ready availability.[19−26] In contrast, reports of nitrogen-containing olefinic monomers such as acylamides, amino-olefins, and acylonitriles are scarce (Figure 1, A−C), since *N*-groups inhibit chain propagation and induce chain transfer far more severely than *O*-groups, resulting in low molecular weight and low comonomer incorporations that seldom exceed 5 mol %.[27−42] Notably, nitrogen-containing polyolefins are highly sought after for applications in self-healing materials,[43] antimicrobial applications,[44] and anion-exchange membranes,[45] among others. Consequently, the highly efficient copolymerization of ethylene and nitrogen-containing olefinic monomers to produce nitrogen-containing polyolefins remains an attractive yet challenging goal.

Norbornene (NB)-derived polar monomers, characterized by high ring strain (approximately 27−30 kcal mol^{-1}) and pronounced π-donor properties, have emerged as promising comonomer candidates for addressing the critical challenges, associated with polar-monomer copolymerization.[46−51] Nitrogen-containing polar norbornene derivatives such as amide,[44,52,53] amino,[54] or nitrile-functionalized norbornene comonomers have been developed (Figure 1, A−C).[52] To overcome these obstacles posed by nitrogen-containing comonomers in ethylene copolymerization, we envision two

Received: June 27, 2025
Revised: August 1, 2025
Accepted: August 8, 2025
Published: August 18, 2025

https://doi.org/10.1021/acs.macromol.5c01720
Macromolecules 2025, 58, 9412−9419

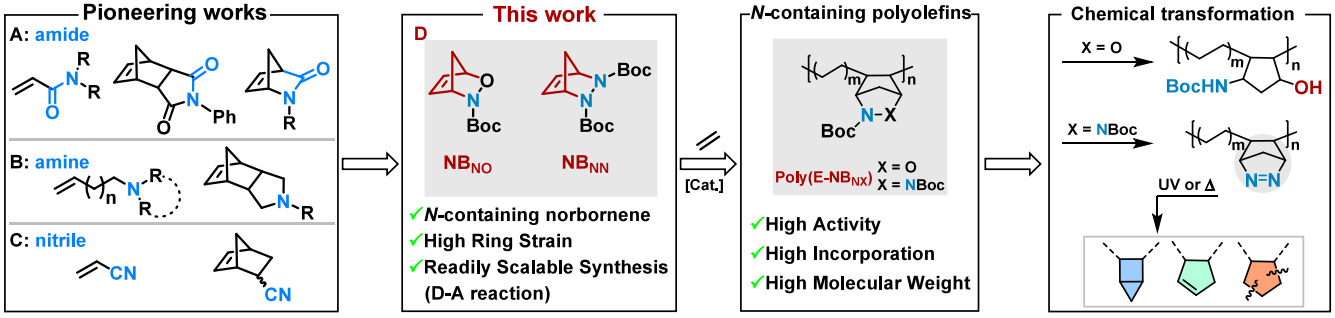

Figure 1. Comparisons of nitrogen-containing olefinic monomers (A–D) used in ethylene copolymerization.

bicyclic heterocycles, in which an aminooxy (N–O) unit or an aza (N–N) unit replaces the nonpolar–CH_2CH_2–bridge in the NB framework, yielding 2-oxa-3-azabicyclo[2.2.1]hept-5-ene ($\mathbf{NB_{NO}}$) and 2,3-diazabicyclo[2.2.1]hept-5-ene ($\mathbf{NB_{NN}}$) (Figure 1, D). On the one hand, the rigid bicyclic scaffold ensures that the ring strain of NB is preserved, thereby promoting efficient copolymerization. As evidence, the ring-opening metathesis polymerization of $\mathbf{NB_{NO}}$ and $\mathbf{NB_{NN}}$ has already been reported.[55,56] On the other hand, embedding the aminooxy/aza nitrogen-containing polar group into the bicyclic backbone—rather than appending it out of norbornene—minimizes the monomer's steric volume and enhances insertion rates, while the methylene bridge combined with bulky amine protecting groups establishes a multidirectional steric shield that averts catalyst deactivation. More notably, aminooxy/aza-embedded norbornenes ($\mathbf{NB_{NO}}$ and $\mathbf{NB_{NN}}$) not only promote ethylene copolymerization to produce nitrogen-containing polyolefins but also facilitate chemical transformation of the obtained polymers to generate diverse polyolefins.[56]

Herein, we for the first time report the coordination–insertion copolymerization of aminooxy/aza-embedding norbornenes, enabling significantly high incorporation of nitrogen-containing functionalities into polyolefins without compromising molecular weight. The high incorporation of $\mathbf{NB_{NO}}$ and $\mathbf{NB_{NN}}$ polar units in the polyolefins permits facile chemical transformations to yield bifunctional polyolefin, azo-containing polyolefin, and diverse all-hydrocarbon cyclo-containing polyolefin architectures.

EXPERIMENTAL METHODS

All of the experimental details involved in the text can be found in the Supporting Information.

RESULTS AND DISCUSSION

Comonomer Design and Synthesis. To prevent catalyst deactivation by free *N*-protons in $\mathbf{NB_{NO}}$ and $\mathbf{NB_{NN}}$, the nitrogen atoms are masked by *tert*-butoxycarbonyl (Boc) groups.[28] $\mathbf{NB_{NO}}$ and $\mathbf{NB_{NN}}$ are synthesized via hetero-Diels–Alder cycloadditions between cyclopentadiene and either an in situ-generated aminooxy dienophile or a Boc-substituted azo dienophile, respectively (Figure 2).[57] During $\mathbf{NB_{NO}}$ synthesis, conventional inorganic oxidants such as sodium periodate ($NaIO_4$) suffer from poor solubility in organic solvents, leading to low reaction rates and extensive side reactions in the heterogeneous oxidation of hydroxylamine precursors. In light of this, we employ tetrabutylammonium periodate [($^nBu_4N$)-IO_4], which combines the strong oxidizing capacity of periodate with the enhanced solubility provided by the tetrabutylammonium cation.[58] As a result, $\mathbf{NB_{NO}}$ and $\mathbf{NB_{NN}}$ are isolated in 85% and 90% yield, respectively (see Figure 4a,b and Figure S3 in Supporting Information). The *tert*-butyl groups derived from Boc are found to confer sufficient lipophilicity to dissolve both comonomers in common organic solvents, including hexane, thus facilitating large-scale purification by recrystallization. Notably, recrystallization of $\mathbf{NB_{NO}}$ from diethyl ether at −30 °C affords colorless crystals, a purity level rarely reported for such analogues.

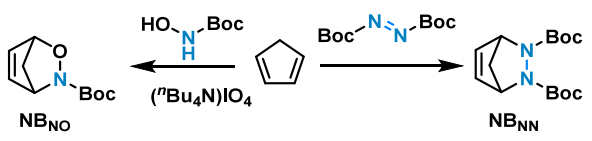

Figure 2. Synthetic pathways of $\mathbf{NB_{NO}}$ and $\mathbf{NB_{NN}}$.

Copolymerization of Ethylene with $\mathbf{NB_{NO}}$ or $\mathbf{NB_{NN}}$. Without activator or scavenger added, phosphine-sulfonate Pd(II) catalysts **Pd1**–**Pd4** with distinct steric bulk[59−63] are synthesized and evaluated in ethylene copolymerization with $\mathbf{NB_{NO}}$ and $\mathbf{NB_{NN}}$ at 8 bar and 80 °C (Table 1). **Pd1** catalyzes the copolymerization of ethylene and $\mathbf{NB_{NO}}$ (0.2 M) for 2 h to afford poly(E-$\mathbf{NB_{NO}}$) with a high $\mathbf{NB_{NO}}$ incorporation of 18.2 mol % (entry 1). This incorporation is comparable to those reported for ester-containing norbornene analogues[46] and significantly exceeds those of linear nitrogen-containing comonomers involved in ethylene copolymerization.[38] As the $\mathbf{NB_{NO}}$ concentration increases from 0.2 to 1.0 M, $\mathbf{NB_{NO}}$ incorporation rises rapidly (entries 1–4); however, both copolymerization activity and copolymer molecular weight first increase and then decrease. Under reduced ethylene pressure (4 bar) or elevated temperature (90 °C), $\mathbf{NB_{NO}}$ incorporation is further enhanced to reach an extreme value of 38.3 mol % (entries 5–7), indicating the effectiveness of aminooxy-embedded norbornene in ethylene copolymerization.

Pd2–**Pd4** also promote ethylene/$\mathbf{NB_{NO}}$ copolymerization but give significantly lower $\mathbf{NB_{NO}}$ incorporations than **Pd1**, with values ranging from one-fifth to two-fifths of that of **Pd1** (entries 8–10 vs entry 4). Notably, **Pd2**, bearing the bulkiest phosphine substituents, yields poly(E-$\mathbf{NB_{NO}}$) with the lowest incorporation (4.6 mol %), **Pd3** even produces only a trace of copolymer, and **Pd4** produces poly(E-$\mathbf{NB_{NO}}$) with middle incorporation (12.7 mol %). These results are indicative of the importance of catalysts used in the copolymerization reaction, albeit with a suitable comonomer.

The copolymerization of ethylene with $\mathbf{NB_{NN}}$ under otherwise identical conditions (**Pd1**, 0.2 M of $\mathbf{NB_{NN}}$, entry 11) yields poly(E-$\mathbf{NB_{NN}}$) with 6.5-fold higher catalytic activity,

https://doi.org/10.1021/acs.macromol.5c01720
Macromolecules 2025, 58, 9412−9419

Table 1. Copolymerization of Ethylene with NB_{NO} or NB_{NN} Using Pd1−Pd4[a]

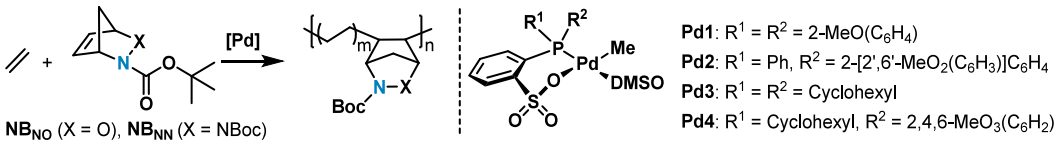

NB_{NO} (X = O), NB_{NN} (X = NBoc)

Entry	T/°C	Cat.	Comonomer (mol L^{-1})	Yield (g)	Act.[b] (10^4)	X_M[c] (mol %)	M_n[d] (10^3)	M_w/M_n[d]	T_g/T_m[e] (°C)
1	80	**Pd1**	NB_{NO} (0.2)	0.54	2.7	18.2	32.0	1.41	58/-
2	80	**Pd1**	NB_{NO} (0.5)	0.49	2.5	26.0	31.9	1.44	90/-
3	80	**Pd1**	NB_{NO} (0.8)	0.71	3.6	27.6	37.1	1.54	107/-
4	80	**Pd1**	NB_{NO} (1.0)	0.60	3.0	29.0	33.3	1.62	110/-
5	90	**Pd1**	NB_{NO} (1.0)	0.55	2.8	31.3	27.0	1.55	118/-
6[f]	80	**Pd1**	NB_{NO} (1.0)	0.55	2.8	37.3	30.6	1.55	135/-
7[f]	90	**Pd1**	NB_{NO} (1.0)	0.41	2.1	38.3	27.7	1.42	141/-
8	80	**Pd2**	NB_{NO} (1.0)	1.78	8.9	6.0	36.9[g]	1.74	-/84
9	80	**Pd3**	NB_{NO} (1.0)	trace	-	-	-	-	-
10	80	**Pd4**	NB_{NO} (1.0)	0.10	0.5	12.7	33.2	1.37	30/-
11	80	**Pd1**	NB_{NN} (0.2)	3.50	17.5	1.8	7.9[g]	2.14	-/127
12	80	**Pd1**	NB_{NN} (0.5)	4.85	24.3	3.9	9.9[g]	2.00	-/126
13	80	**Pd1**	NB_{NN} (0.8)	4.71	23.6	17.6	77.0	1.74	76/120
14	80	**Pd1**	NB_{NN} (1.0)	4.10	20.5	22.0	85.4	1.77	94/-
15	90	**Pd1**	NB_{NN} (1.0)	3.40	17.0	24.2	77.3	1.75	102/-
16[f]	80	**Pd1**	NB_{NN} (1.0)	2.42	12.1	28.3	108.1	1.73	115/-
17[f]	90	**Pd1**	NB_{NN} (1.0)	2.20	11.0	31.4	87.9	1.83	132/-
18	80	**Pd2**	NB_{NN} (1.0)	2.50	12.5	4.6	21.4[g]	1.88	-/91
19	80	**Pd3**	NB_{NN} (1.0)	0.33	1.7	13.6	56.2	1.35	62/-
20	80	**Pd4**	NB_{NN} (1.0)	0.40	2.0	13.0	72.6	1.33	60/-

[a]Reaction conditions: Pd(II) catalysts (10 μmol), polymerization temperature (80 °C), toluene (20 mL), ethylene (8 bar), unless noted otherwise. [b]Activity is in unit of g mol^{-1} h^{-1}. [c]Determined by ^1H NMR spectroscopy. X_M = Incorporation of polar monomer. [d]Determined by GPC in THF at 40 °C against a polystyrene standard. [e]Determined by DSC at 10 K min^{-1} (second heating). [f]Ethylene (4 bar). [g]Determined by GPC in 1,2,4-trichlorobenzene at 150 °C using a refractive index detector.

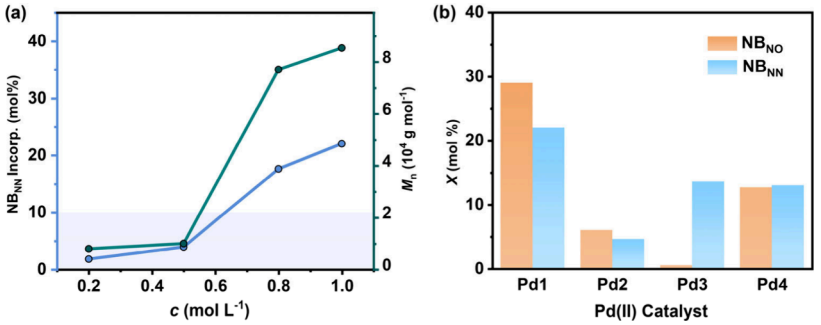

Figure 3. (a) Plots of the M_n and comonomer incorporation of poly(E-NB_{NN}) generated versus comonomer concentration with **Pd1** (8 bar, 2 h, 80 °C). (b) Comparative analysis of NB_{NO} versus NB_{NN} incorporation in ethylene copolymerization catalyzed by Pd(II) catalysts (1.0 mol L^{-1}, 8 bar, 2 h, and 80 °C).

but with only 1.8 mol % incorporation and a low molecular weight (7.9 × 10^3 g mol^{-1}), revealing that increased steric bulk of comonomer diminishes catalyst poisoning of NB_{NN} versus NB_{NO} (entry 1 vs entry 11). Gradually elevating the NB_{NN} concentration from 0.2 to 1.0 M leads to a notably simultaneous increase in incorporation and molecular weight, with the effect particularly pronounced between 0.5 and 0.8 M (entries 11−14; Figure 3a). We attribute this trend to the enhanced solubility of the growing copolymer, which promotes polymerization, and to the substantial molecular weight difference between NB_{NN} and ethylene (296.37 g mol^{-1} vs 28 g mol^{-1}). Reducing ethylene pressure (4 bar) or raising polymerization temperature (90 °C) leads to higher NB_{NN} incorporation (up to 31.4 mol %) and copolymer molecular weight (up to 87.9 × 10^3 g mol^{-1}). Meanwhile, **Pd1** maintains high catalytic activity on the order of 1 × 10^5 g mol^{-1} h^{-1} over the entire concentration range, reflecting the high ring strain and negligible poisoning effect of NB_{NN}. Among **Pd2−Pd4**, **Pd2** again exhibits the lowest incorporation (4.6 mol % at 1.0 M), whereas **Pd3** and **Pd4** afford moderate incorporations (13.0−13.6 mol %) but display lower activities, consistent with trends observed for NB_{NO}-involving copolymerization (Figure 3b).

A side-by-side comparison of the two comonomers reveals that a single Boc group in NB_{NO} provides inadequate steric shielding, leading to significant catalyst deactivation, especially at higher comonomer concentrations (>0.8 M). Consequently, both copolymerization activity and copolymer molecular

https://doi.org/10.1021/acs.macromol.5c01720
Macromolecules 2025, 58, 9412−9419

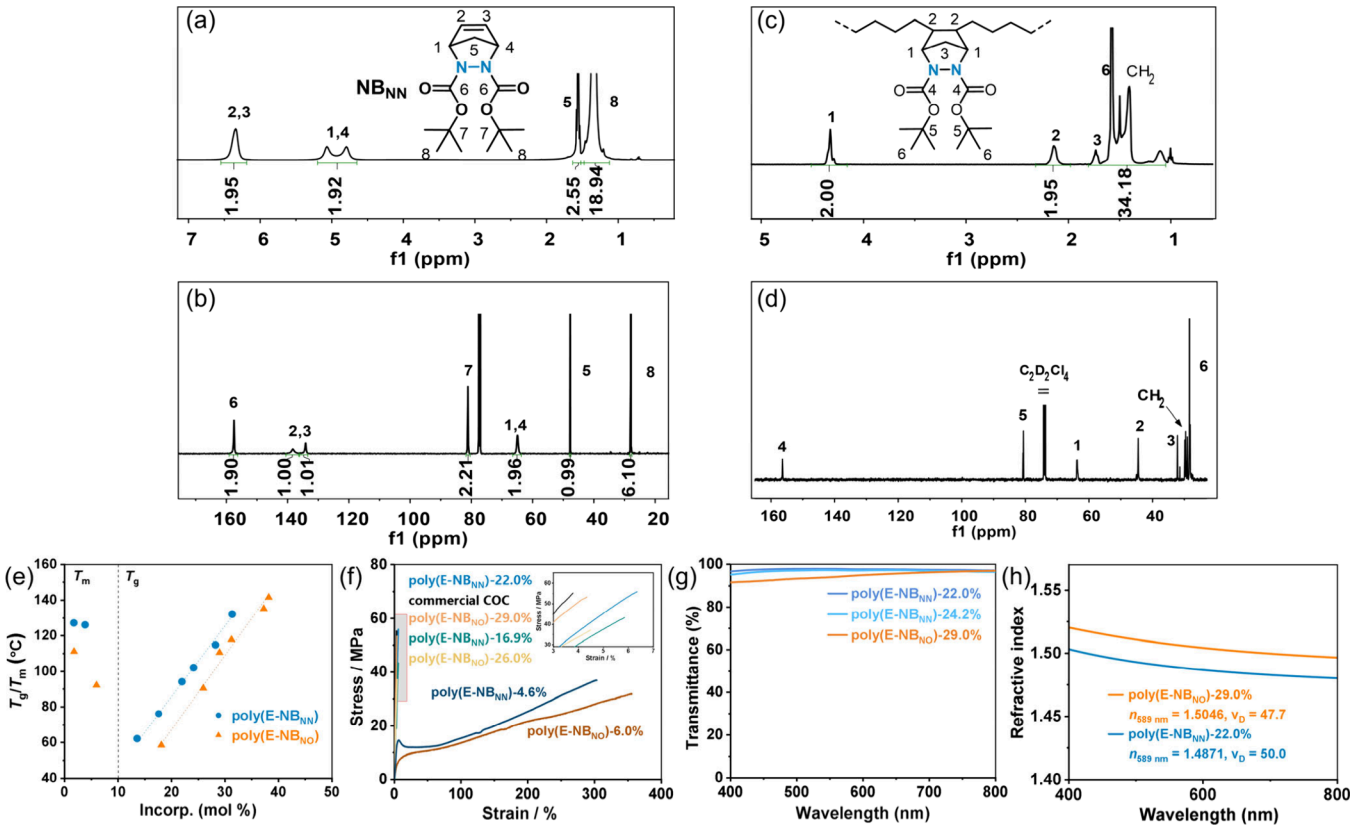

Figure 4. (a) ^{1}H NMR spectrum of $\mathbf{NB_{NN}}$ in $CDCl_3$. (b) ^{13}C NMR spectrum of $\mathbf{NB_{NN}}$ in $CDCl_3$. (c) ^{1}H NMR spectrum of poly(E-$\mathbf{NB_{NN}}$)-22.0% in $C_2D_2Cl_4$ (Table 1, entry 14). (d) ^{13}C NMR spectrum of poly(E-$\mathbf{NB_{NN}}$)-22.0% in $C_2D_2Cl_4$ (Table 1 entry 14). (e) Relationship of T_g/T_m with the comonomer incorporation. (f) Stress−strain curves of copolymers with different incorporations. (g) Optical transmittance of copolymer samples. (h) Refractive indices of copolymer samples at 400−800 nm.

weight are markedly lower than those achieved with $\mathbf{NB_{NN}}$, despite $\mathbf{NB_{NO}}$'s relatively high incorporation. In contrast, the amine groups of $\mathbf{NB_{NN}}$ are flanked by a methylene bridge and two bulky Boc substituents, forming a three-dimensional steric barrier that effectively suppresses deactivation, thereby permitting high comonomer incorporation without compromising the activity and polymer molecular weight.

Structure and Property of Nitrogen-Containing Polyolefins. The microstructures and properties of poly(E-$\mathbf{NB_{NO}}$) and poly(E-$\mathbf{NB_{NN}}$) are thoroughly characterized by ^{1}H and ^{13}C NMR spectroscopy, infrared spectroscopy (IR), differential scanning calorimetry (DSC), UV/vis spectrometry, and tensile testing (Figure 4; Supporting Information). In the ^{1}H NMR spectrum of poly(E-$\mathbf{NB_{NN}}$), broad resonances—distinct from the sharp signals of $\mathbf{NB_{NN}}$—mirror those observed in ethylene/norbornene copolymers [COC: poly(E-NB)]. In particular, the broad resonance at δ = 2.14 ppm arises from the−CH−CH−motif of inserted $\mathbf{NB_{NN}}$ (Figure 4c), a finding corroborated by the ^{13}C NMR signal at δ = 44.52 ppm (peak 2 in Figure 4d). Sharp ^{13}C resonances for carbons 1−6 of the inserted NB_{NN} unit confirm its isolated, nonconsecutive insertion rather than block or alternating sequences, and the Boc carbonyl appears at δ = 156.39 ppm, further validating the copolymer structure. IR spectroscopy further corroborates the copolymer structure with the Boc carbonyl stretch observed at 1695 cm^{-1} (Figure S80).

DSC curves underscore the significant impact of inserted $\mathbf{NB_{NN}}$ unit on the thermal behavior of the corresponding copolymers: as shown in Figure 4e, poly(E-$\mathbf{NB_{NN}}$) samples prepared with **Pd1** exhibit melting endotherms (T_m = 126−127 °C) at low $\mathbf{NB_{NN}}$ contents (≤3.9 mol %), indicative of the presence of long, crystalline polyethylene segments. With increasing $\mathbf{NB_{NN}}$ incorporation, the glass transition temperature linearly rises, in line with established trends for cyclic-olefin copolymers, reaching a maximum of T_g = 132 °C at 31.4 mol %. By contrast, nonpolar poly(E-NB) copolymers with the similar norbornene content display T_g values of only 70−80 °C [empirically T_g = 2.66(NB %)−11.3],[64] highlighting the markedly enhanced heat resistance of poly(E-$\mathbf{NB_{NN}}$). Interestingly, comparative DSC analysis of poly(E-$\mathbf{NB_{NO}}$) and poly(E-$\mathbf{NB_{NN}}$) samples exhibits that, at the same comonomer incorporation (31.3 vs 31.4 mol %), T_g (118 °C) of poly(E-$\mathbf{NB_{NO}}$) is clearly lower than that of poly(E-$\mathbf{NB_{NN}}$) (132 °C), highlighting the impact of comonomer architecture on polymer properties.

Given their high comonomer incorporations and molecular weights, poly(E-$\mathbf{NB_{NO}}$) and poly(E-$\mathbf{NB_{NN}}$) are evaluated for mechanical performance (Figure 4f). Poly(E-$\mathbf{NB_{NN}}$) with 4.6 mol % of incorporation exhibits a tensile strength of 36.8 MPa and an elongation at break of 303%, on par with conventional polyethylene. As $\mathbf{NB_{NN}}$ incorporation increases, tensile strength rises while elongation falls, ultimately approaching that of commercial cyclic-olefin copolymer (COC) ($\sigma \approx 55$ MPa, $\varepsilon \approx 3\%$).[65] Notably, poly(E-$\mathbf{NB_{NN}}$) with 22.0 mol % incorporation reaches σ = 55.9 MPa and ε = 6%, indicating that the introduction of a polar group can partially alleviate the inherent brittleness of COC; likewise, poly(E-$\mathbf{NB_{NO}}$) with 29.0 mol % incorporation attains σ = 53.3 MPa and ε = 4%.

https://doi.org/10.1021/acs.macromol.5c01720
Macromolecules 2025, 58, 9412−9419

COC materials are widely used as optical plastics;[65] therefore, the visible-light transmittance of amorphous poly(E-$\mathbf{NB}_{NO}$) and poly(E-$\mathbf{NB}_{NN}$) films is measured over 400−800 nm range (Figure 4g). Poly(E-$\mathbf{NB}_{NN}$) samples with 22.0 and 24.2 mol % incorporation have particularly high transparency of 96.6% and 95.2% at 400 nm, respectively, while poly(E-$\mathbf{NB}_{NO}$) with 29.0 mol % incorporation transmits 91.5%. This enhanced transparency reflects the effects of the incorporated polar groups.[66] Refractive-index and optical-dispersion measurements (Figure 4h) show that poly(E-$\mathbf{NB}_{NO}$) and poly(E-$\mathbf{NB}_{NN}$) exhibit promising optical properties [poly(E-$\mathbf{NB}_{NO}$)-29.0%, n_{589} = 1.5046, ν_D = 47.7; poly(E-$\mathbf{NB}_{NN}$)-22.0%, n_{589} = 1.4871, ν_D = 50.0]. As a result, polyethylenes with high incorporation of nitrogen-containing norbornene act as good optical material.

Chemical Transformations of Poly(E-$\mathbf{NB}_{NO}$) and Poly(E-$\mathbf{NB}_{NN}$). Polyolefins typically exhibit poor solubility, hindering efficient chemical transformation. In contrast, poly(E-$\mathbf{NB}_{NO}$) and poly(E-$\mathbf{NB}_{NN}$) bearing >10 mol % polar comonomer units dissolve readily at room temperature in common organic solvents such as dichloromethane, thus enabling facile modification. Furthermore, the presence of cyclic nitrogen-containing units supports diverse postfunctionalization reactions (Figure 5).

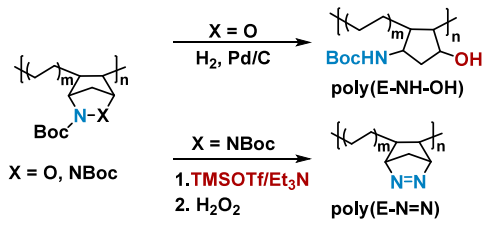

Figure 5. Chemical transformations of poly(E-$\mathbf{NB}_{NO}$) and poly(E-$\mathbf{NB}_{NN}$).

Catalytic hydrogenolysis of the N−O bond in poly(E-$\mathbf{NB}_{NO}$) with Pd/C at 110 °C cleanly produces the desired bifunctional poly(E-NH−OH).[67] However, strong hydrogen-bonding between the polar groups makes this polymer insoluble in common solvents.[56] IR analysis confirms the generation of free hydroxyl and amine functionalities, with a broad O−H/N−H stretching band appearing at 3364 cm^{-1} and a single carbonyl absorption at 1698 cm^{-1} replacing the original doublet in poly(E-$\mathbf{NB}_{NO}$) (Figure S79, S81). Similarly, deprotection of Boc in poly(E-$\mathbf{NB}_{NN}$) using trifluoroacetic acid or KOH at elevated temperatures results in immediate gelation and precipitation, which undermines complete deprotection and precludes further modification. We attribute this to intermolecular hydrogen bonding between the newly formed N−H sites. After multiple attempts, treatment of poly(E-$\mathbf{NB}_{NN}$)-28.3% with neutral trimethylsilyl trifluoromethanesulfonate (TMSOTf) at room temperature for 48 h achieved quantitative Boc removal without precipitation. Subsequent in situ oxidation of the liberated amine groups with hydrogen peroxide yields the azo-functionalized polyolefin [poly(E-N═N)]. These meticulously regulated postfunctionalization processes exemplify the distinctive potential of aminooxy/aza-functionalized polyolefins derived from $\mathbf{NB}_{NO}$ and $\mathbf{NB}_{NN}$.

Poly(E−N═N) is comprehensively characterized by $^1H/^{13}C$ NMR spectroscopy, infrared spectroscopy (IR), differential scanning calorimetry (DSC), thermogravimetric analysis (TGA), and GC−MS. A signal appearing at δ = 4.94 ppm in the ^1H NMR spectrum (Figure 6a, peak 1) provides clear evidence of N═N bond formation, further corroborated by associated ^{13}C resonances at δ = 80.52 ppm (Figure 6b, peak 1). IR additionally verifies the azo moiety via the N═N stretching band at 1498 cm^{-1} (Figure 6c). DSC traces indicate that the T_g of poly(E-N═N) (111 °C) is slightly lower than that of the corresponding poly(E-$\mathbf{NB}_{NN}$) (114 °C) (Figure 6d). TGA analysis shows that poly(E-N═N) exhibits nitrogen-releasing behavior: the first decomposition begins at 201 °C and the mass-loss ratio matches the azo content in the incorporated comonomer (Figure 6e). GC−MS analysis confirms nitrogen to be the evolved gas. These combined data establish poly(E−N═N) as a novel thermally triggered nitrogen-releasing polymer (Figure 6f).

Chemical Transformation of Poly(E−N═N). The N_2-extrusion reaction of the azo functionality can be driven thermally or photochemically via a cyclopentane diradical intermediate, enabling construction of diverse polyolefin architectures by simple adjustment of reaction conditions (Figure 7). Under air at 250 °C, direct heating of poly(E-N═N) yields poly(E-N═N)-cross-link: the complete disappearance of the N═N stretching band at 1498 cm^{-1} in the IR spectrum confirms azo bond cleavage and network formation (Figure 7d).[68] By contrast, under an argon atmosphere in deuterated tetrachloroethane ($C_2D_2Cl_4$) with UV irradiation (λ = 365 nm for 1.5 h), the rearrangement of radicals can be regulated. At room temperature, the cyclopentane diradical rearranges preferentially to cyclopentene [poly(E-CP)], as evidenced by the appearance of olefinic ^1H signals at δ = 5.84 and 5.72 ppm (Figure 7b).[69] Lowering the temperature to 0 °C favors intramolecular coupling of the diradical to facilitate bicyclic frameworks [poly(E-BCP)],[70] confirmed by two sets of characteristic methylene proton resonances at δ = 0.64/0.31 ppm and 0.72/0.57 ppm for the exo and endo BCP units, respectively. Furthermore, the chemical shifts align with those obtained in analogous small-molecule studies (Figure 7c).[69] These results suggest an interesting transformation from azo-containing polyolefins to all-hydrocarbon cyclo-containing (3-, 4-, 5-membered ring) polyolefins, which are difficult to be accessed by other methods.

CONCLUSIONS

In summary, this work establishes a versatile nitrogen-containing olefinic comonomer design approach for the highly efficient copolymerization of nitrogen-containing monomers with ethylene. This so-called aminooxy/aza-embedded norbornenes serve as ideal comonomers that mitigate *N*-induced catalyst poisoning, enabling the significantly higher incorporation of *N*-functions into polyolefins without compromising the molecular weight while retaining high catalytic activity. This balance of catalytic activity, polymer molecular weight, and comonomer incorporation has been sought-after over decades. The broad range of varied comonomer incorporations alters nitrogen-containing polyolefins [poly(E-$\mathbf{NB}_{NO}$) and poly(E-$\mathbf{NB}_{NN}$)] from semicrystalline polymer to amorphous optical polymer. This notably higher comonomer incorporation is comparable to those in oxygen-containing polyolefins and importantly increases the solubility of nitrogen-rich polyolefins and thus enables facile chemical transformation. This results in the formation of NH/OH-bifunctional poly(E-NH−OH) and an azo-containing polyolefin [poly(E-N═N)]. Furthermore, thermally/photochemically driven chemical

https://doi.org/10.1021/acs.macromol.5c01720
Macromolecules 2025, 58, 9412−9419

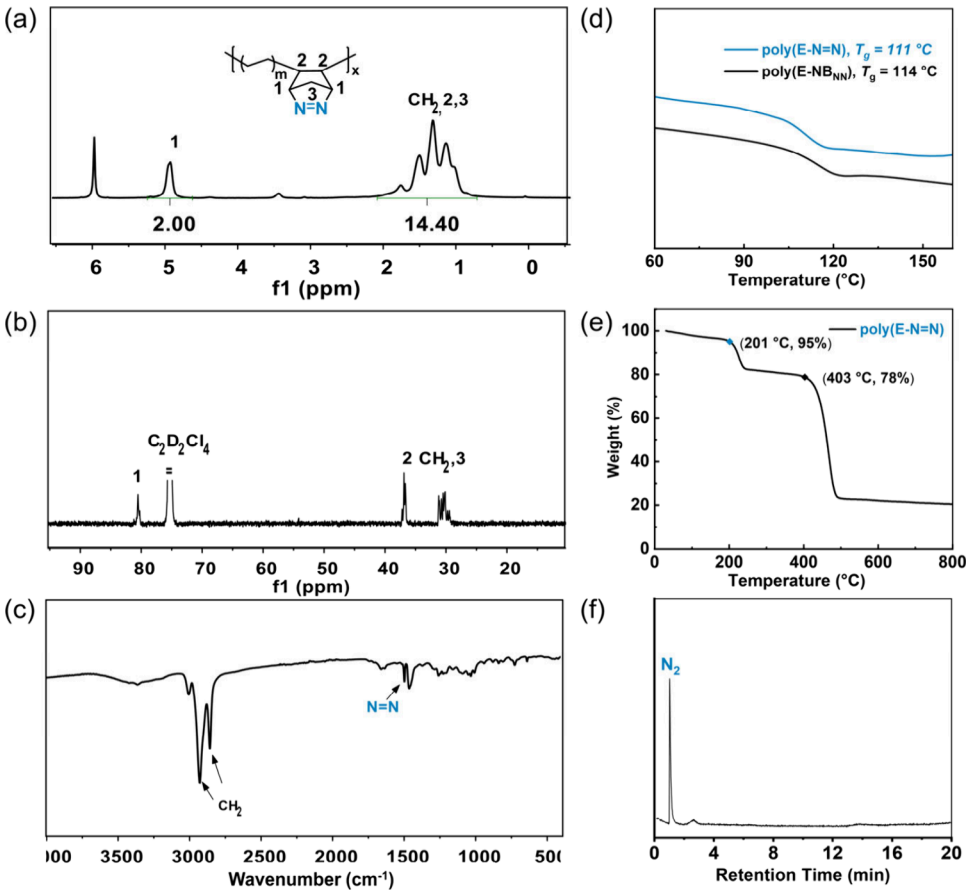

Figure 6. (a) ^{1}H NMR spectrum of poly(E-N═N)-27.7% in $C_2D_2Cl_4$. (b) ^{13}C NMR spectrum of poly(E-N═N)-27.7% in $C_2D_2Cl_4$. (c) IR spectrum of poly(E-N═N)-27.7%. (d) DSC curves of poly(E-**NB**$_{NN}$)-28.3% and poly(E-N═N)-27.7%. (e) TGA curve of poly(E-N═N)-27.7%. (f) Gas chromatogram of poly(E-N═N)-27.7% at 250 °C.

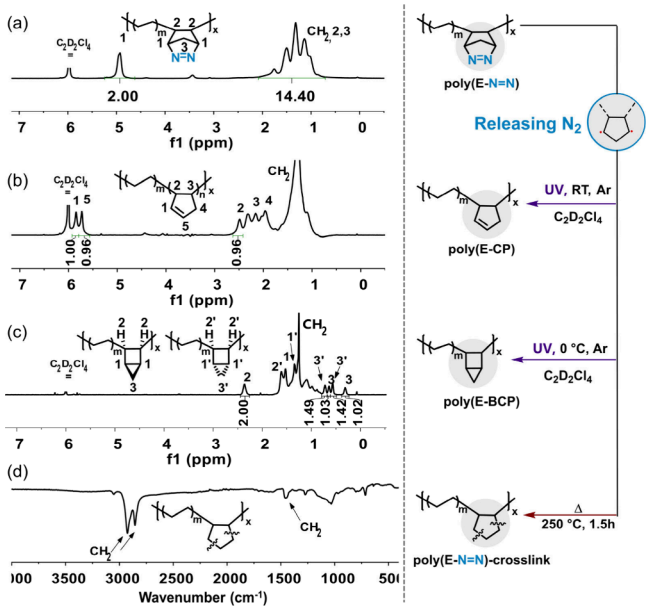

Figure 7. (a) ^{1}H NMR spectrum of poly(E-N═N)-27.7% in $C_2D_2Cl_4$. (b) ^{1}H NMR spectrum of poly(E-CP) in $C_2D_2Cl_4$. (c) ^{1}H NMR spectrum of poly(E-BCP) in $C_2D_2Cl_4$. (d) IR spectrum of poly(E-N═N)-cross-link.

transformation of poly(E-N═N) gives all-hydrocarbon cyclo-containing polyolefins. These polyolefins originated from chemical transformation are difficult to access by other methods. This work thus presents a general comonomer design strategy for accessing multifunctional, nitrogen-rich polyolefins.

■ ASSOCIATED CONTENT

Supporting Information

The Supporting Information is available free of charge at https://pubs.acs.org/doi/10.1021/acs.macromol.5c01720.

General procedure and comonomer preparation; characterization and analytical data (NMR, DSC, and GPC) for comonomers and copolymers (PDF)

■ AUTHOR INFORMATION

Corresponding Authors

Yixin Zhang − *State Key Laboratory of Polymer Science and Technology, Changchun Institute of Applied Chemistry, Chinese Academy of Sciences, Changchun 130022, China*; Email: zhangyixin@ciac.ac.cn

Zhongbao Jian − *State Key Laboratory of Polymer Science and Technology, Changchun Institute of Applied Chemistry, Chinese Academy of Sciences, Changchun 130022, China*; orcid.org/0000-0002-2627-454X; Email: zbjian@ciac.ac.cn

https://doi.org/10.1021/acs.macromol.5c01720
Macromolecules 2025, 58, 9412−9419

Authors

Kangkang Li − *State Key Laboratory of Polymer Science and Technology, Changchun Institute of Applied Chemistry, Chinese Academy of Sciences, Changchun 130022, China*

Lei Cui − *State Key Laboratory of Polymer Science and Technology, Changchun Institute of Applied Chemistry, Chinese Academy of Sciences, Changchun 130022, China*

Complete contact information is available at: https://pubs.acs.org/10.1021/acs.macromol.5c01720

Notes

The authors declare no competing financial interest.

■ ACKNOWLEDGMENTS

We are thankful for financial support from National Key R&D Program of China (No. 2022YFB3607400), National Natural Science Foundation of China (No. U23B6011), Jilin Provincial Science and Technology Department Program (No. 20250102080JC), and Youth Innovation Promotion Association CAS Program (No. 2023235).

■ REFERENCES

(1) Hustad, P. D. Frontiers in Olefin Polymerization: Reinventing the World's Most Common Synthetic Polymers. *Science* **2009**, *325*, 704−707.

(2) Stürzel, M.; Mihan, S.; Mülhaupt, R. From Multisite Polymerization Catalysis to Sustainable Materials and All-Polyolefin Composites. *Chem. Rev.* **2016**, *116*, 1398−1433.

(3) Baier, M. C.; Zuideveld, M. A.; Mecking, S. Post-Metallocenes in the Industrial Production of Polyolefins. *Angew. Chem., Int. Ed.* **2014**, *53*, 9722−9744.

(4) Zhang, Y.; Zhang, Y.; Hu, X.; Wang, C.; Jian, Z. Advances on controlled chain walking and suppression of chain transfer in catalytic olefin polymerization. *ACS Catal.* **2022**, *12*, 14304−14320.

(5) Nakamura, A.; Ito, S.; Nozaki, K. Coordination−insertion copolymerization of fundamental polar monomers. *Chem. Rev.* **2009**, *109*, 5215−5244.

(6) Chen, Z.; Brookhart, M. Exploring ethylene/polar vinyl monomer copolymerizations using Ni and Pd α-diimine Catalysts. *Acc. Chem. Res.* **2018**, *51*, 1831−1839.

(7) Chen, C. Designing catalysts for olefin polymerization and copolymerization: beyond electronic and steric tuning. *Nature Reviews Chemistry* **2018**, *2*, 6−14.

(8) Luckham, S. L. J.; Nozaki, K. Toward the copolymerization of propylene with polar comonomers. *Acc. Chem. Res.* **2021**, *54*, 344−355.

(9) Mu, H.; Jian, Z. Stereoselective copolymerization of olefin with polar monomers to access stereoregular functionalized polyolefins. *Organic Materials* **2022**, *4*, 178−189.

(10) Mu, H.; Pan, L.; Song, D.; Li, Y. Neutral Nickel catalysts for olefin homo- and copolymerization: relationships between catalyst structures and catalytic properties. *Chem. Rev.* **2015**, *115*, 12091−12137.

(11) Tan, C.; Chen, C. Emerging palladium and nickel catalysts for copolymerization of olefins with polar monomers. *Angew. Chem., Int. Ed.* **2019**, *58*, 7192−7200.

(12) Keyes, A.; Basbug Alhan, H. E.; Ordonez, E.; Ha, U.; Beezer, D. B.; Dau, H.; Liu, Y.; Tsogtgerel, E.; Jones, G. R.; Harth, E. Olefins and vinyl polar monomers: bridging the gap for next generation materials. *Angew. Chem., Int. Ed.* **2019**, *58*, 12370−12391.

(13) Chen, J.; Gao, Y.; Marks, T. J. Early Transition Metal Catalysis for Olefin-Polar Monomer Copolymerization. *Angew. Chem., Int. Ed.* **2020**, *59*, 14726−14735.

(14) Mecking, S.; Schnitte, M. Neutral Nickel(II) catalysts: from hyperbranched oligomers to nanocrystal-based materials. *Acc. Chem. Res.* **2020**, *53*, 2738−2752.

(15) Mu, H.; Zhou, G.; Hu, X.; Jian, Z. Recent advances in nickel mediated copolymerization of olefin with polar monomers. *Coord. Chem. Rev.* **2021**, *435*, No. 213802.

(16) Zhou, G.; Cui, L.; Mu, H.; Jian, Z. Custom-made polar monomers utilized in nickel and palladium promoted olefin copolymerization. *Polym. Chem.* **2021**, *12*, 3878−3892.

(17) Tan, C.; Zou, C.; Chen, C. Material properties of functional polyethylenes from transition-metal-catalyzed ethylene−polar monomer copolymerization. *Macromolecules* **2022**, *55*, 1910−1922.

(18) Yang, Q.; Kang, X.; Liu, Y.; Mu, H.; Jian, Z. Ultrahigh Molecular Weight Ethylene-Acrylate Copolymers Synthesized with Highly Active Neutral Nickel Catalysts. *Angew. Chem., Int. Ed.* **2025**, *64*, No. e202421904.

(19) Zheng, H.; Qiu, Z.; Li, D.; Pei, L.; Gao, H. Advance on nickel- and palladium-catalyzed insertion copolymerization of ethylene and acrylate monomers. *J. Polym. Sci.* **2023**, *61*, 2987−3021.

(20) Xiong, S.; Shoshani, M. M.; Zhang, X.; Spinney, H. A.; Nett, A. J.; Henderson, B. S.; M, T. F., III; Agapie, T. Efficient Copolymerization of Acrylate and Ethylene with Neutral P, O-Chelated Nickel Catalysts: Mechanistic Investigations of Monomer Insertion and Chelate Formation. *J. Am. Chem. Soc.* **2021**, *143*, 6516−6527.

(21) Xiong, S.; Hong, A.; Bailey, B. C.; Spinney, H. A.; Senecal, T. D.; Bailey, H.; Agapie, T. Highly Active and Thermally Robust Nickel Enolate Catalysts for the Synthesis of Ethylene-Acrylate Copolymers. *Angew. Chem., Int. Ed.* **2022**, *61*, No. e202206637.

(22) Xiong, S.; Hong, A.; Ghana, P.; Bailey, B. C.; Spinney, H. A.; Bailey, H.; Henderson, B. S.; Marshall, S.; Agapie, T. Acrylate-Induced β-H Elimination in Coordination Insertion Copolymerizaton Catalyzed by Nickel. *J. Am. Chem. Soc.* **2023**, *145*, 26463−26471.

(23) Xiong, S.; Spinney, H. A.; Bailey, B. C.; Henderson, B. S.; Tekpor, A. A.; Espinosa, M. R.; Saha, P.; Agapie, T. Switchable Synthesis of Ethylene/Acrylate Copolymers by a Dinickel Catalyst: Evidence for Chain Growth on Both Nickel Centers and Concepts of Cation Exchange Polymerization. *ACS Catal.* **2024**, *14*, 5260−5268.

(24) Ghana, P.; Xiong, S.; Tekpor, A.; Bailey, B. C.; Spinney, H. A.; Henderson, B. S.; Agapie, T. Catalyst Editing via Post-Synthetic Functionalization by Phosphonium Generation and Anion Exchange for Nickel-Catalyzed Ethylene/Acrylate Copolymerization. *J. Am. Chem. Soc.* **2024**, *146*, 18797−18803.

(25) Ito, S.; Munakata, K.; Nakamura, A.; Nozaki, K. Copolymerization of Vinyl Acetate with Ethylene by Palladium/Alkylphosphine−Sulfonate Catalysts. *J. Am. Chem. Soc.* **2009**, *131*, 14606−14607.

(26) Luo, S.; Vela, J.; Lief, G. R.; Jordan, R. F. Copolymerization of Ethylene and Alkyl Vinyl Ethers by a (Phosphine- sulfonate)PdMe Catalyst. *J. Am. Chem. Soc.* **2007**, *129*, 8946−8947.

(27) Skupov, K. M.; Piche, L.; Claverie, J. P. Linear polyethylene with tunable surface properties by catalytic copolymerization of ethylene with N-Vinyl-2-pyrrolidinone and N-Isopropylacrylamide. *Macromolecules* **2008**, *41*, 2309−2310.

(28) Zou, C.; Zhang, H.; Tan, C.; Cai, Z. Polyolefins with intrinsic antimicrobial properties. *Macromolecules* **2021**, *54*, 64−70.

(29) Zhang, Y.; Mu, H.; Pan, L.; Wang, X.; Li, Y. Robust Bulky [P,O] Neutral Nickel Catalysts for Copolymerization of Ethylene with Polar Vinyl Monomers. *ACS Catal.* **2018**, *8*, 5963−5976.

(30) Xia, J.; Zhang, Y.; Hu, X.; Ma, X.; Cui, L.; Zhang, J.; Jian, Z. Sterically very bulky aliphatic/aromatic phosphine-sulfonate palladium catalysts for ethylene polymerization and copolymerization with polar monomers. *Polym. Chem.* **2019**, *10*, 546−554.

(31) Chen, J.; Gao, Y.; Wang, B.; Lohr, T. L.; Marks, T. J. Scandium-Catalyzed Self-Assisted Polar Co-monomer Enchainment in Ethylene Polymerization. *Angew. Chem., Int. Ed.* **2017**, *56*, 15964−15968.

(32) Chen, J.; Motta, A.; Wang, B.; Gao, Y.; Marks, T. J. Significant Polar Comonomer Enchainment in Zirconium-Catalyzed, Masking Reagent-Free. *Ethylene Copolymerizations. Angew. Chem. Int. Ed.* **2019**, *58*, 7030−7034.

(33) Huang, M.; Chen, J.; Wang, B.; Huang, W.; Chen, H.; Gao, Y.; Marks, T. J. Polar Isotactic and Syndiotactic Polypropylenes by

Organozirconium-Catalyzed Masking-Reagent-Free Propylene and Amino−Olefin Copolymerization. *Angew. Chem., Int. Ed.* **2020**, *59*, 20522−20528.
(34) Wang, C.; Luo, G.; Nishiura, M.; Song, G.; Yamamoto, A.; Luo, Y.; Hou, Z. Heteroatom-assisted olefin polymerization by rare-earth metal catalysts. *Science Advances* **2017**, *3*, No. e1701011.
(35) Zhang, Z.; Jiang, Y.; Lei, R.; Zhang, Y.; Li, S.; Cui, D. Proximity-Driven Synergic Copolymerization of Ethylene and Polar Monomers. *Macromolecules* **2023**, *56*, 2476−2483.
(36) Shang, R.; Gao, H.; Luo, F.; Li, Y.; Wang, B.; Ma, Z.; Pan, L.; Li, Y. Functional Isotactic Polypropylenes via Efficient Direct Copolymerizations of Propylene with Various Amino-Functionalized α-Olefins. *Macromolecules* **2019**, *52*, 9280−9290.
(37) Yu, S. Y.; Wang, X. Y.; Sun, X. L.; Gao, Y.; Zhao, Y.; Ning, X. S.; Ji, G.; Lu, Y.; Yang, J.; Liu, Z. P.; Tang, Y. Cyano-functionalized polyethylenes from ethylene/acrylamide copolymerization. *Nat. Commun.* **2025**, *16*, 2461.
(38) Friedberger, T.; Wucher, P.; Mecking, S. Mechanistic insights into polar monomer insertion polymerization from acrylamides. *J. Am. Chem. Soc.* **2012**, *134*, 1010−1018.
(39) Stehling, U. M.; Stein, K. M.; Kesti, M. R.; Waymouth, R. M. Metallocene/Borate-Catalyzed Polymerization of Amino-Functionalized α-Olefins. *Macromolecules* **1998**, *31*, 2019−2027.
(40) Schneider, M. J.; Schäfer, R.; Mülhaupt, R. Aminofunctional linear low density polyethylene via metallocene-catalysed ethene copolymerization with N,N-bis(trimethylsilyl)-1-amino-10-undecene. *Polymer* **1997**, *38*, 2455−2459.
(41) Stehling, U. M.; Malmström, E. E.; Waymouth, R. M.; Hawker, C. J. Synthesis of Poly(olefin) Graft Copolymers by a Combination of Metallocene and "Living" Free Radical Polymerization Techniques. *Macromolecules* **1998**, *31*, 4396−4398.
(42) Kochi, T.; Noda, S.; Yoshimura, K.; Nozaki, K. Formation of Linear Copolymers of Ethylene and Acrylonitrile Catalyzed by Phosphine Sulfonate Palladium Complexes. *J. Am. Chem. Soc.* **2007**, *129*, 8948−8949.
(43) Yavitt, B. M.; Tomkovic, T.; Gilmour, D. J.; Zhang, Z.; Kuanr, N.; van Ruymbeke, E.; Schafer, L. L.; Hatzikiriakos, S. G. Rheology and self-healing of amine functionalized polyolefins. *J. Rheol.* **2022**, *66*, 1125−1137.
(44) Li, K.; Cui, L.; Zhang, Y.; Jian, Z. Amide-functionalized polyolefins and facile post-transformations. *Macromolecules* **2023**, *56*, 915−922.
(45) Park, E. J.; Jannasch, P.; Miyatake, K.; Bae, C.; Noonan, K.; Fujimoto, C.; Holdcroft, S.; Varcoe, J. R.; Henkensmeier, D.; Guiver, M. D.; Kim, Y. S. Aryl ether-free polymer electrolytes for electrochemical and energy devices. *Chem. Soc. Rev.* **2024**, *53*, 5704−5780.
(46) Ravasio, A.; Boggioni, L.; Tritto, I. Copolymerization of ethylene with norbornene by neutral aryl phosphine sulfonate Palladium catalyst. *Macromolecules* **2011**, *44*, 4180−4186.
(47) Schuster, N.; Rünzi, T.; Mecking, S. Reactivity of functionalized vinyl monomers in insertion copolymerization. *Macromolecules* **2016**, *49*, 1172−1179.
(48) Xu, M.; Chen, C. A disubstituted-norbornene-based comonomer strategy to address polar monomer problem. *Sci. Bull.* **2021**, *66*, 1429−1436.
(49) Wang, W.; Chen, M.; Pang, W.; Li, Y.; Zou, C.; Chen, C. Palladium-catalyzed synthesis of norbornene-based polar-functionalized polyolefin elastomers. *Macromolecules* **2021**, *54*, 3197−3203.
(50) Pasini, D.; Takeuchi, D. Cyclopolymerizations: synthetic tools for the precision synthesis of macromolecular architectures. *Chem. Rev.* **2018**, *118*, 8983−9057.
(51) Xu, M.; Chen, A.; Li, W.; Li, Y.; Zou, C.; Chen, C. Efficient synthesis of polar functionalized polyolefins with high biomass content. *Macromolecules* **2023**, *56*, 1372−1378.
(52) Na, Y.; Zhang, D.; Chen, C. Modulating polyolefin properties through the incorporation of nitrogen-containing polar monomers. *Polym. Chem.* **2017**, *8*, 2405−2409.
(53) Chen, M.; Chen, C. Rational design of high-performance phosphine sulfonate nickel catalysts for ethylene polymerization and copolymerization with polar monomers. *ACS Catal.* **2017**, *7*, 1308−1312.
(54) Dong, S.; Cai, L.; Han, Z.; Liu, B.; Cui, D. CGC-Scandium-Mediated Copolymerization of Ethylene with Amine-Functionalized Cyclic Olefins. *ACS Catal.* **2024**, *14*, 15565−15571.
(55) Mandal, A.; Kilbinger, A. F. M. Catalytic Living ROMP: Synthesis of Degradable Star Polymers. *ACS Macro Lett.* **2023**, *12*, 1372−1378.
(56) Subnaik, S.; Sheridan, K.; Hobbs, C. E. Ring opening metathesis polymerization of a new monomer derived from a nitroso Diels−Alder reaction. *Macromol. Chem. Phys.* **2021**, *222*, 2100098.
(57) Zhang, Y.; Jermaks, J.; MacMillan, S. N.; Lambert, T. H. Synthesis of 2H-Chromenes via Hydrazine-Catalyzed Ring-Closing Carbonyl-Olefin Metathesis. *ACS Catal.* **2019**, *9*, 9259−9264.
(58) Durham, R.; Mandel, J.; Blanchard, N.; Tam, W. Ruthenium-catalyzed [2 + 2] cycloaddition reactions of a 2-oxa-3-azabicyclo[2.2.1]hept-5-ene with unsymmetrical alkynes. *Can. J. Chem.* **2011**, *89*, 1494−1505.
(59) Guironnet, D.; Roesle, P.; Rünzi, T.; Göttker-Schnetmann, I.; Mecking, S. Insertion polymerization of acrylate. *J. Am. Chem. Soc.* **2009**, *131*, 422−423.
(60) Ito, S.; Kanazawa, M.; Munakata, K.; Kuroda, J.; Okumura, Y.; Nozaki, K. Coordination−insertion copolymerization of allyl monomers with ethylene. *J. Am. Chem. Soc.* **2011**, *133*, 1232−1235.
(61) Na, Y.; Dai, S.; Chen, C. Direct synthesis of polar-functionalized linear low-density polyethylene (LLDPE) and low-density polyethylene (LDPE). *Macromolecules* **2018**, *51*, 4040−4048.
(62) Wucher, P.; Goldbach, V.; Mecking, S. Electronic influences in phosphinesulfonato Palladium(II) polymerization catalysts. *Organometallics* **2013**, *32*, 4516−4522.
(63) Piche, L.; Daigle, J.; Rehse, G.; Claverie, J. P. Structure−activity relationship of Palladium phosphanesulfonates: toward highly active Palladium-based polymerization catalysts. *Chem.—Eur. J.* **2012**, *18*, 3277−3285.
(64) Wang, B.; Tang, T.; Li, Y.; Cui, D. Copolymerization of ethylene with norbornene catalyzed by cationic rare earth metal fluorenyl functionalized N-heterocyclic carbene complexes. *Dalton Trans.* **2009**, 8963−8969.
(65) Hong, M.; Cui, L.; Liu, S.; Li, Y. Synthesis of novel cyclic olefin copolymer (COC) with high performance via effective copolymerization of ethylene with bulky cyclic olefin. *Macromolecules* **2012**, *45*, 5397−5402.
(66) Sun, N.; Yi, C.; Xu, C.; Xu, J.; Ma, M.; Shi, Y.; He, H.; Zhu, Y.; Chen, S.; Wang, X. Fabrication of Permanent Antistatic PMMA Copolymer for Enhanced Antistatic and Mechanical Properties. *ACS Appl. Polym. Mater.* **2023**, *5*, 5537−5543.
(67) Kulagowski, J. J.; Blair, W.; Bull, R. J.; Chang, C.; Deshmukh, G.; Dyke, H. J.; Eigenbrot, C.; Ghilardi, N.; Gibbons, P.; Harrison, T. K.; Hewitt, P. R.; Liimatta, M.; Hurley, C. A.; Johnson, A.; Johnson, T.; Kenny, J. R.; Bir Kohli, P.; Maxey, R. J.; Mendonca, R.; Mortara, K.; Murray, J.; Narukulla, R.; Shia, S.; Steffek, M.; Ubhayakar, S.; Ultsch, M.; van Abbema, A.; Ward, S. I.; Waszkowycz, B.; Zak, M. Identification of imidazo-pyrrolopyridines as novel and potent JAK1 inhibitors. *J. Med. Chem.* **2012**, *55*, 5901−5921.
(68) Enholm, E.; Joshi, A.; Wright, D. L. Photocurable hard and porous biomaterials from ROMP precursors cross-linked with diyl radicals. *Bioorg. Med. Chem. Lett.* **2005**, *15*, 5262−5265.
(69) Sarkar, S. K.; Solel, E.; Kozuch, S.; Abe, M. Heavy-Atom Tunneling Processes during Denitrogenation of 2,3-Diazabicyclo[2.2.1]hept-2-ene and Ring Closure of Cyclopentane-1,3-diyl Diradical. Stereoselectivity in Tunneling and Matrix Effect. *J. Org. Chem.* **2020**, *85*, 8881−8892.
(70) Zhang, X.; Zhao, Y.; Chen, M.; Ji, M.; Sha, Y.; Nozaki, K.; Tang, S. Polyethylene Materials with Tunable Degradability by Incorporating In-Chain Mechanophores. *J. Am. Chem. Soc.* **2024**, *146*, 24024−24032.

https://doi.org/10.1021/acs.macromol.5c01720
Macromolecules 2025, 58, 9412−9419